

## EVALUATION OF ADHESION STRENGTH IN CONCRETE WITH CRACK INDUCED DUE TO STEEL CORROSION BY NONDESTRUCTIVE TESTING

Yuto Nakagawa<sup>1</sup> Shinichi Miyazato<sup>2</sup> Kentaro Ohno<sup>3</sup>

<sup>1</sup> Graduate student, Kanazawa Institute of Technology, 3-1, Yatsukaho, Hakusan-shi, Ishikawa 924-0838, Japan

<sup>2</sup> Professor, Kanazawa Institute of Technology, 3-1, Yatsukaho, Hakusan-shi, Ishikawa 924-0838, Japan

<sup>3</sup> Assistant Professor, Tokyo Metropolitan University, 1-1, Minami-Osawa, Hachioji-shi, Tokyo

### ARTICLE INFO:

*Received: October 8, 2018*

*Received Revised Form:*

*October 24, 2018*

*Accepted: October 25, 2018*

### ABSTRACT:

Currently, it is regarded as a problem that aged structures are rapidly increasing in maintenance of RC members. Therefore, it is desirable to integrate rational inspection and repair for aged RC members in maintenance. In other words, it is ideal to first conduct a standard investigation for a wide area in a short time and then to examine the degree of deterioration in detail at a limited range. Therefore, it is necessary to consider the corrosion of the steel bar which serves as the nucleus in the maintenance control against chloride attack, and the adhesion characteristics between the steel bar and the concrete decreased thereby. However, a quantitative and systematic estimation method has not been established for the steel corrosion in RC members. Therefore, in this study, specimens having several degrees of steel corrosion were prepared within the range where no cracks appeared on the surface. A combination of nondestructive testing was conducted to estimate the adhesion strength between steel bars and concrete. The degree of steel corrosion was estimated first by the half-cell potential, then internal cracks due to steel corrosion in concrete were visually investigated by ultrasonic tomography method. As a result of this experiment, it was possible to identify the corroded area was specified with the half-cell potential. Moreover, as corrosion progressed, it became clear that the ultrasonic velocity around the steel bar decreased, and the adhesion strength between the steel bar and the concrete decreased. Therefore, this study could develop a maintenance method combining the half-cell potential and the ultrasonic tomography method.

*\*Corresponding Author,*

*Email address:*

*b1422933@planet.kanazawa-it.ac.jp*

**KEYWORDS:** Half-cell Potential, Ultrasonic Testing, Steel Corrosion, Internal Crack, Adhesion Stress

## 1. Introduction

Currently, it is regarded as a problem that aged structures are rapidly increasing in Japan. Therefore, it is desirable to integrate rational inspection and repair for RC members. In other words, it is ideal to conduct a standard investigation for a wide area in a short time and then to examine a deterioration in detail at a limited area. Here, corrosion due to chloride attack causes volumetric expansion of the steel bar, and generates micro cracks in concrete around the corroded steel bar [1,2]. As a result, an adhesion between the steel bar and the concrete may decrease[3,4]. However, a quantitative and systematic estimation method for the deterioration of the adhesion characteristics between the steel bar and the concrete has not been established both domestically and overseas [5].

The use of nondestructive testing has been widely expanded in recent years, and the results of them give some advantage information for diagnosis in concrete structures. In particular, ultrasonic testing has been applied on deteriorated concrete structures to estimate damage degree. Herein, cracks in due to a steel corrosion in concrete cannot be visually observed. In such situation, because the ultrasonic velocity would decrease due to micro cracks in concrete, presence of the induced cracks due to a steel corrosion can be estimated. In addition, the velocity decreasing area can be visually and easily observed by a tomography technique.

In this paper, based on the above background, two steps approaches by nondestructive testing were conducted to estimate a steel corrosion and the presence of corrosion-induced cracks in concrete. In the experiment, specimens were prepared, which had 4 different degrees of steel corrosion by controlling the period of electrolytic corrosion.

The steel corrosion degree in a specimen was monitored by employing the half-cell potential. Then, ultrasonic testing was applied to the specimen after electrolytic corrosion test. The presence of the cracks due to steel corrosion in the specimen was estimated by the ultrasonic velocity distribution of tomography method. After that, an adhesion stress between the steel bar and the concrete in the specimen was obtained by pulling a corroded steel bar. Finally the relationships of these indicators were discussed.

## 2. Experimental procedure

### 2.1 Specimen

The configuration of specimens is shown in Figure 1, and the mixture proportion of concrete is shown in Table 1. Ordinary Portland cement was used for cement, and W/C of concrete was 55%. In addition, the specimen was a rectangular parallelepiped of  $200 \times 200 \times 150$  (mm), and three steel bars (D 13, SD 345) were embedded. Only the center steel bar was set to 800 mm to carry out the adhesion test.

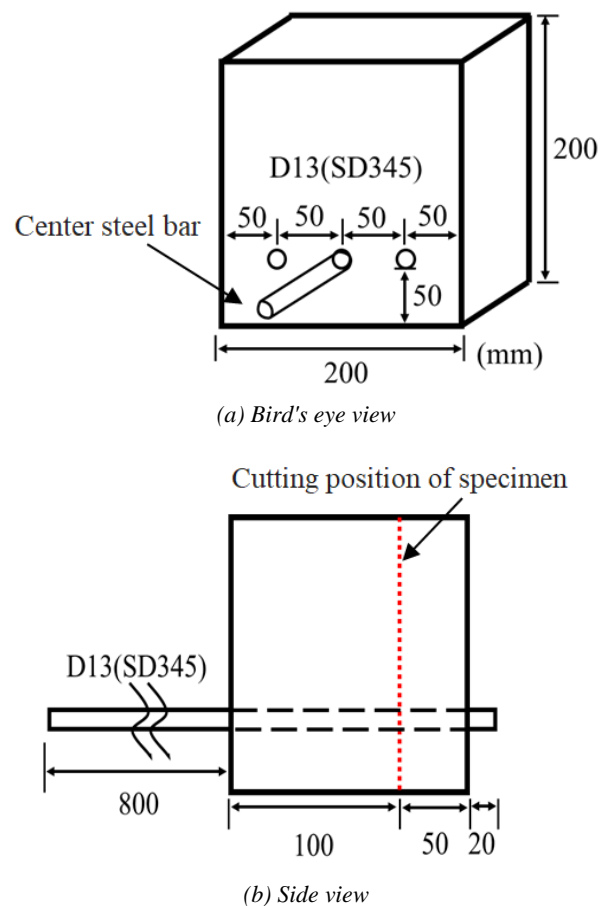


**Figure 1** Specimen overview.

**Table 1** Summary of crack condition on RC2

W/C (%)	s/a (%)	Unit weight(kg/m <sup>3</sup> )			
		W	C	S	G
55	41.75	175	318	759	1046

## 2.2 Set-up of degree of steel corrosion

The degree of steel corrosion are listed in Table 2. In this experiment, the assuming of use of a nondestructive testing would be set for a situation where any deterioration cannot be visually observed from the surface of concrete. Therefore, the degree of corrosion progression was mainly set to specimens that surface cracks did not generate on the concrete surface. In this study as a feasibility study, the electrolytic corrosion was applied to the specimens because the steel corrosion can be accelerated and easy to control that degree. Here, it seems that corrosion expansion phenomenon of steel bars are different between the electrolytic and chloride corruptions. Therefore, additional experiments with chloride attacks will be carried out in the future. The diagram of the electrolytic corrosion is shown in Figure 2. Based on some literatures [6-8], a 3% sodium chloride aqueous solution was used as the electrolytic solution. Furthermore, the center steel bar in three steel bars was set as an anode, a copper plate placed on a surface of the specimen as a cathode, and a current of 0.25 A was energized. Four degrees of corrosion situations were set, and the energization periods were set to 0, 48, 96 and 115 hours, respectively. When the energization period was just 115 hours, cracks were visually observed at the cover concrete. Specimens were set drying condition (20 °C, RH 60%) for 1 day from the end of the electrolytic corrosion until measurements with a half-cell potential and an ultrasonic tomography. In Case 1, the cover concrete was immersed in water after initial curing. Thereafter, the specimen was stored at a dry environment (20 °C, RH 60%) until measurements.

**Table 2** Degree of steel corrosion

Case	Degree of corrosion progression	Energization periods (hour)
1	Nothing	0
2	Small	48
3	Large	96
4	Excess	115

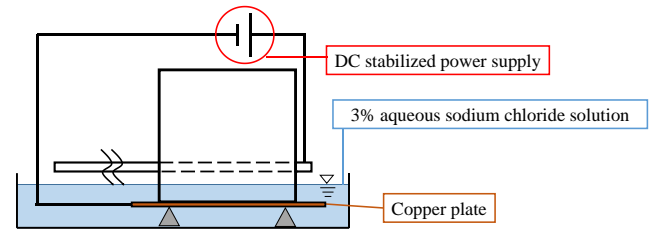


**Figure 2** Electrolytic corrosion of specimen.

## 2.3 Measuring method

### (1) Visual inspection

The damage degree in specimens was investigated at cover concrete by visual inspection. As a result, deterioration condition in concrete was confirmed.

### (2) Half-cell potential

After the specimen was set the dry condition, the half-cell potential was measured at the center steel bar with Ag/AgCl as a reference electrode in order to ascertain the possibility of corrosion. After the measurement, it was converted to the value for CSE (saturated copper sulfate). As a result, the corrosion state of the steel bar could be checked, and if it was an actual structure, the deterioration level could be grasped.

### (3) Ultrasonic testing

To estimate the presence of internal cracks due to corrosion expansion of steel bar, the ultrasonic velocity was measured. Therefore, tomographic analysis [9] is performed using the propagation time difference between each sensor, and the distribution of ultrasonic velocity in the specimen was investigated. The array of AE sensors is shown in Figure 3. 15 AE sensors of 60 kHz resonance frequency were attached to the specimen surface at intervals of 40 mm. The amplitude of the emitted pulse signal was 15 V, this signal was transformed one AE sensor, then propagated waves were detected by other 14 AE sensors. Detected waves were amplified with 40 dB by pre-amplifiers. Then one waveform was AD converted at a sampling frequency of 1 MHz (sampling interval 1 μs) and recorded. By processing the signal obtained in this way, the state inside the specimen was estimated from ultrasonic information.

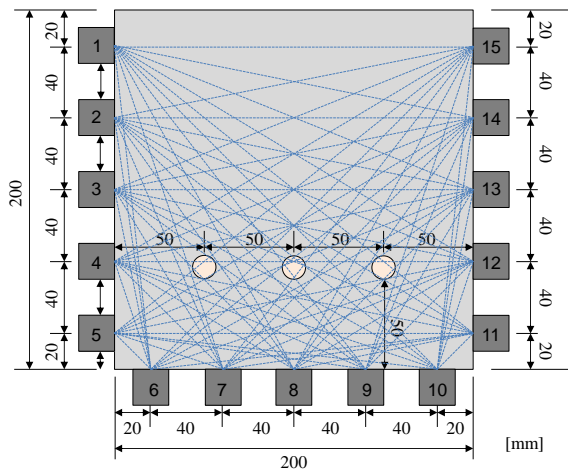


**Figure 3** Array of AE sensors for tomography.

#### (4) Internal crack observation by visual inspection

In order to check the presence of internal cracks due to the steel corrosion, cracks between steel bars were visually inspected from the outside of the specimen. Furthermore, the specimen was cut with a concrete cutter at the dotted line portion in Figure 1. And the internal cracks around the steel bar was observed using a digital microscope (magnification: 25 times).

#### (5) Adhesion test

Adhesion strength between the steel bar and the concrete was measured after above inspections according to JSCE-G 503-2010. The adhesion strength was obtained to divide the tensile load by the surface area of the steel bar in the test section. Here the circumferential length of the steel bar was taken as the nominal value of a sound steel bar. The test outline is shown in Figure 4. The target is the center steel bar.

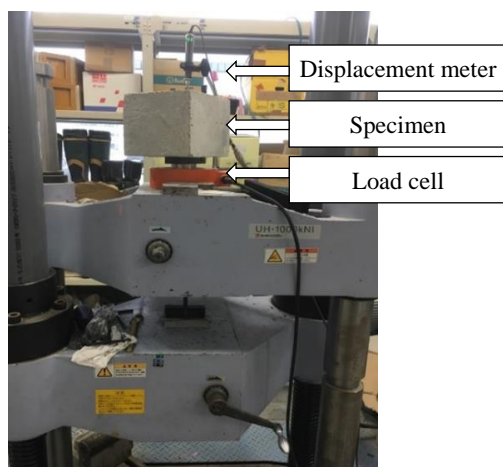


**Figure 4** Adhesion test.

### 3. Experimental result

#### 3.1 Visual inspection at whole specimen

In cases 1-3, surface cracks did not generate at the specimen surface. On the other hand, in Case 4, a crack along the center steel bar was observed.

#### 3.2 Half-cell Potential

The results of the half-cell potential are shown in Figure 5. The progress of corrosion increased as increasing the degree of the steel corrosion. The potential of steel corrosion shifted to negative value. According to this figure, it can be seen that the steel corrosion is progressing. Regarding the possibility of steel corrosion, according to the criteria of ASTM, when CSE reference electrode is used, the steel bar would not be corroded when the potential is over -200 mV, while a possibility of the steel corrosion would be higher when the potential is under -350 mV [10]. Comparing this criteria with the measured values, it can be judged that the steel bar in Cases 2 ~ Case 4 were corroded with a probability of 90% or more.

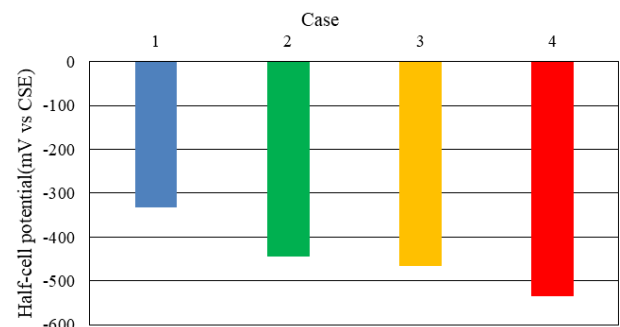


**Figure 5** Result of half-cell potential.

#### 3.3 Result of ultrasonic tomography analysis

The results of ultrasonic tomography analysis at the cross section in concrete are shown in Figure 6. In all specimens, the ultrasonic velocity is relatively low at the side surfaces near 1CH to 5CH and 11 CH to 15 CH. This reason seems to be that the sensor distance at side surfaces in the specimen is as short as 40 mm and the sampling time resolution of the measuring equipment is 1  $\mu$ s in this experiment. Therefore, it is necessary to devise measures to eliminate these effects.

Next, in case 1, case 2, and case 3, ultrasonic velocities at the cover concrete were almost similar (6CH to 10CH bonded surface). However, in Case 4, the low velocity area appears in the cover concrete. This reason seems to be that the ultrasonic velocity

decreases because cracks due to the steel corrosion occurred around the steel bar only in Case 4.

Here, Figure 8 shows the average value of the ultrasonic velocities for the elements near the corroded steel bar shown in Figure 7. According to Figure 8, it can be found that as the corrosion progresses, the ultrasonic velocity around the steel bar decreases even though very little.

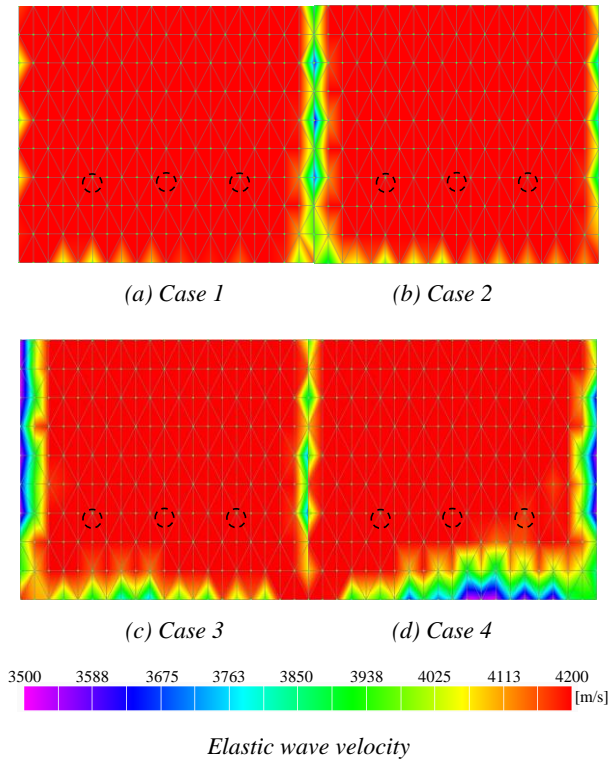


**Figure 6** Result of ultrasonic tomography analysis (15 sensor).

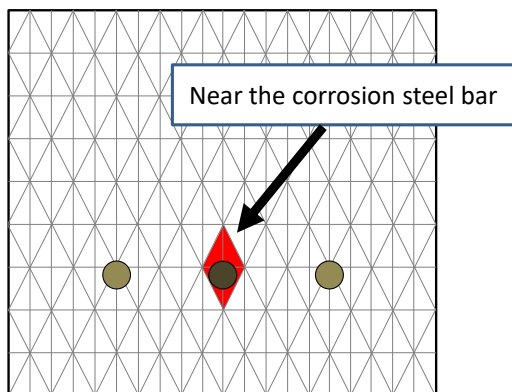


**Figure 7** Elements near corroded steel bar.

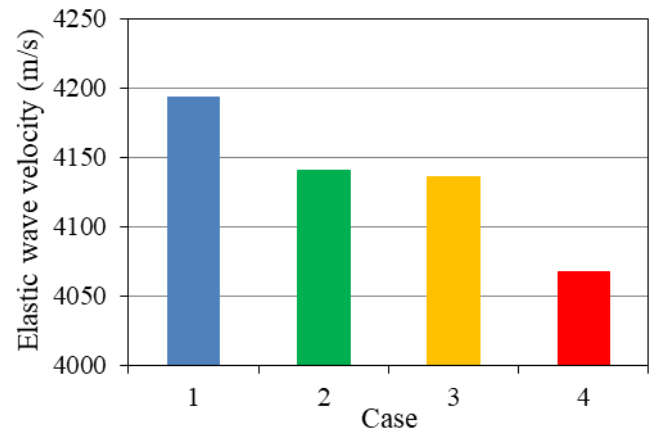


**Figure 8** Average value of ultrasonic velocities at Figure 7 (15 sensor).

As a result of the above investigation, it is a problem that the reliability of the ultrasonic velocity between the sensors in the short distance is low. Therefore, the ultrasonic velocity between the sensors attached on the same side was assumed to be the same as the velocity obtained between 1 CH-15 CH, and the other velocities were used as obtained. That is, the considerable sensors are shown in Figure 9. The result of elastic wave tomography analysis obtained from these information is shown in Figure 10. According to Figure 10, it can be seen that as the corrosion progresses, the area of the low velocity region extends from the bottom cover concrete toward the top of the specimen. Figure 11 shows the average values of ultrasonic velocities at the elements in the vicinity of the corroded steel bar shown in Figure 7. According to Figure 11, it can be confirmed that as the corrosion progresses, the ultrasonic velocity around the steel bar decreases even though very minute.

From the above results, it is considered that it is possible to visualize the decrease of the ultrasonic velocity using the ultrasonic tomography method, and to judge whether the presence of cracks due to the steel corrosion.



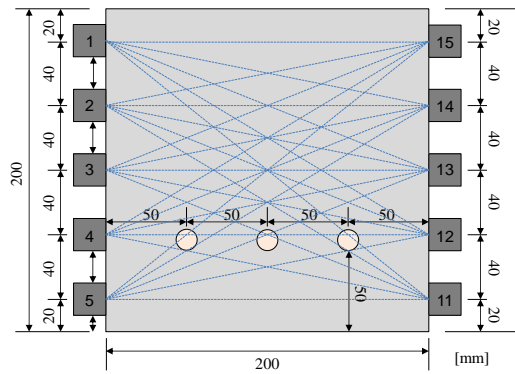


**Figure 9** Attachment positions of AE sensor.

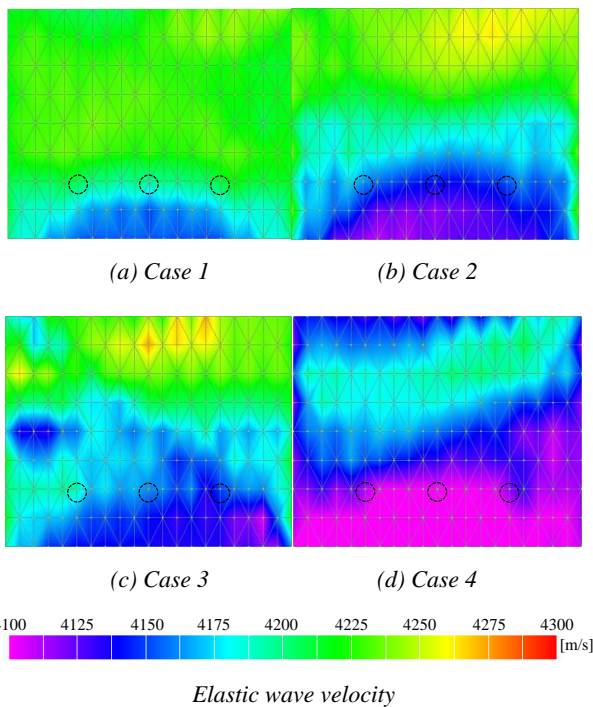


**Figure 10** Result of ultrasonic tomography analysis (10 sensor).

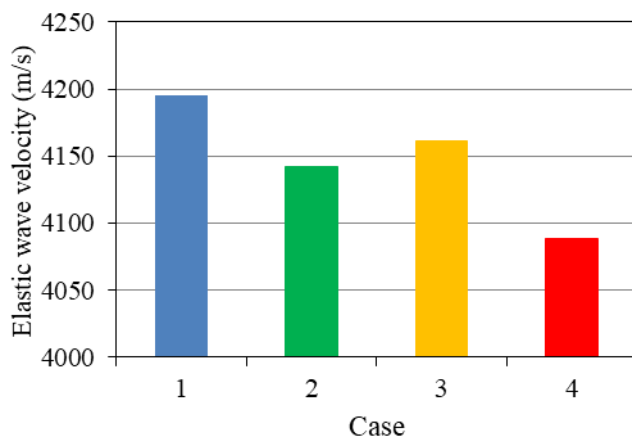
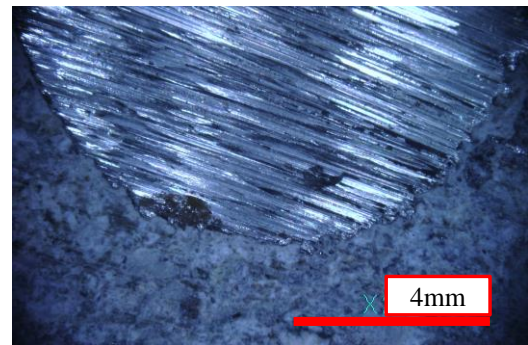


**Figure 11** Average value of ultrasonic velocities at Figure 10 (10 sensor).

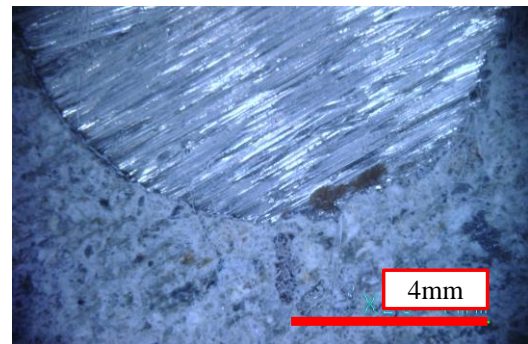
### 3.4 Visual inspection at vicinity of corrode steel bar

The specimen was cut with the concrete cutter and the side surface was visually examined to observe the situation of internal cracks. As a result, there is not an internal crack in Cases 1~3. On the other hand, in Case 4, it can be confirmed that there are the lateral direction cracks from the center steel bar to the steel bar at both ends similar to the literature [1]. The width of this lateral direction crack is 0.1 mm.

Next, a digital microscope observation was carried out in order to observe cracks due to steel corrosion at vicinity of the corrode steel bar. The vicinity area of the corrode steel bar at the cross section in Case 2 and Case 3 are shown in Figure 12. According to these figures, there is rust leachate from the steel bars. However, because the magnification is low, it is impossible to observe a fine internal crack.



(a) Case 2



(b) Case 3

**Figure 12** Result of digital microscope.

### 3.5 Adhesion test

In all cases, the specimens were broken by adhesion splitting. The results of the maximum adhesion stress are shown in Figure 13. The adhesion stress decreases as progresses of the steel corrosion.

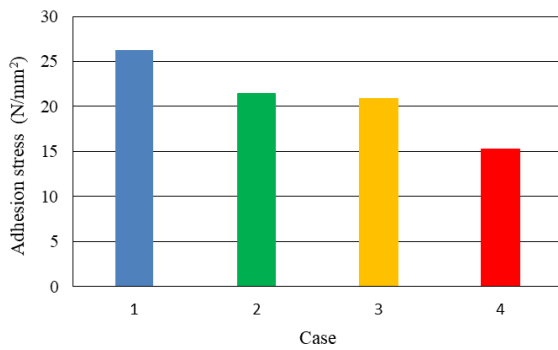


Figure 13 Maximum adhesion stress.

#### 4. Adhesion evaluation by combination of nondestructive tests

The results of the nondestructive tests and the adhesion stress are summarized in Table 3. It is found that the potential, the ultrasonic velocity, and the adhesion stress decrease as the corrosion progresses. Next, the relationship between the ultrasonic velocities and the adhesion stress is shown in Figure 14 and Figure 15. It can be seen that as the ultrasonic velocity decreases due to the steel corrosion, the adhesion stress decreases. Therefore, a proportional relationship between the ultrasonic velocity and the adhesion stress was clearly obtained during progressive on the steel corrosion.

Based on the above experimental results, this paper proposes a method to estimate an adhesion force between the steel bar and concrete in maintenance for chloride attack of RC members. First of all, a standard survey of a wide area in a short time is conducted by using a relatively easy half-cell potential method. As a result, it can be obtained where a steel corrosion progresses. Then, at the limited where the steel corrosion is proceeding, the ultrasonic tomography method is applied to visualize the distribution of ultrasonic velocity inside concrete. The results of the ultrasonic tomography bring information that internal cracks are generated around the steel bar. Furthermore, based on Figure 14 and Figure 15, the adhesion force between the steel bar and concrete could be estimated. Since these figures are different depending on the diameter of the steel bar, the size of the cover concrete and the mixture proportion of concrete, an additional research is necessary.

Table 3 Results of nondestructive tests and adhesion stress

Case	Nondestructive tests			Adhesion stress (N/mm <sup>2</sup> )
	Half-cell potential (mV vs CSE)	Ultrasonic velocity (m/s)		
		15 sensor	10 sensor	
1	-333	4194	4195	26.22
2	-443	4141	4142	21.41
3	-465	4136	4161	20.92
4	-534	4068	4089	15.31

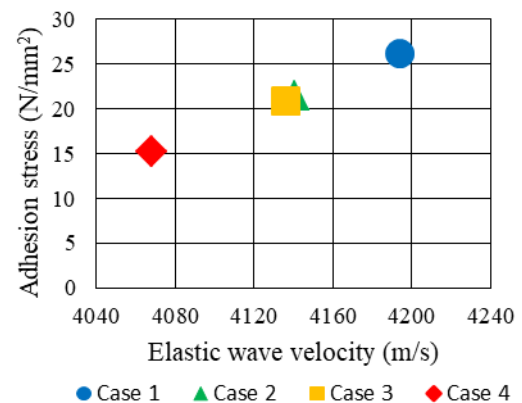


Figure 14 Relationship between ultrasonic velocity (15 sensor) and adhesion.

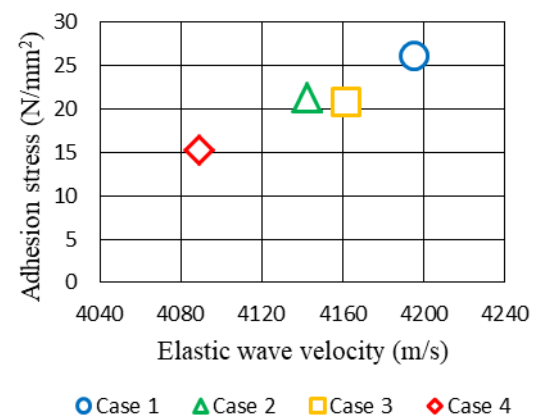


Figure 15 Relationship between ultrasonic velocity (10 sensor) and adhesion.

## 5. Summary

The main findings obtained in this study are described below.

(1) A method to estimate the adhesion stress between a steel bar and concrete is proposed by a combination of nondestructive tests, when micro cracks occurs around the steel bars due to corrosion although cracks does not generate in the concrete surface. In this method, first, the area of the steel corrosion is investigated by the half-cell potential, and then the reduction of the ultrasonic velocity around the steel corroded bar by the ultrasonic tomography method is recognized. By this procedure, the degree of the adhesion stress between a steel bar and concrete could be estimated.

(2) In this experiment using specimens with different corrosion progression, the ultrasonic velocity around the steel bar and the adhesion strength between the steel bar and concrete has a proportional relationship.

## 6. Acknowledgements

It was carried out as part of Grant-in-Aid for Science Research No. 17H0328900.

## 7. Reference

- [1] T. Tsutsumi, M. Matushima, Y. Murakami, and H. Seki, "Study on crack models caused by pressure due to corrosion products," Proceedings of Japan Society of Civil Engineers, No.532/V-30, pp.159-166, 1996.
- [2] M. Tsunomoto, Y. Kajikawa, and M. Kawamura, "Elasto-plastic analysis of expansive behavior due to corrosion of reinforcement," Proceedings of Japan Society of Civil Engineers, Vol.402, pp.151-159, 1989.
- [3] Y. Goto, and K. Otsuka, "Experimental studies on cracks formed in concrete around deformed tension bars," Proceedings of Japan Society of Civil Engineers, Vol.284, pp.85-100, 1980.
- [4] M. Kurumatani, Y. Nemoto, S. Okazaki, and S. Hirose, "Simulation of crack-paths formed in concrete around deformed tension bar," Transactions of the Japan Society for Computational Engineering and Science, No.20140008, 2014.
- [5] Japan Society of Civil Engineering, "Maintenance priority of concrete structure causing material deterioration subcommittee (342 Committee (Phase 2)) committee result report," Concrete technology series 110, p.23, 2015.
- [6] Y. Kawasaki, M. Kitaura, Y. Tomoda, and M. Ohtsu, "Corrosion process in reinforced concrete identified by acoustic emission," Proceedings of Japan Society of Civil Engineers, Vol.67, No.3, pp.384-395, 2011.
- [7] H. Mae, T. Kamada, H. Minesawa, and S. Uchida, "Application of nondestructive testing for evaluation of deterioration around rebar in concrete," Proceedings of the Japan Concrete Institute, Vol.30, No.2, pp.811-816, 2008.
- [8] K. Kawamura, H. Nakamura, M. Kunieda, and N. Ueda, "Fundamental study on evaluation of crack propagation behavior of concrete with steel corrosion," Proceedings of the Japan Concrete Institute, Vol.30, No.2, pp.1075-1080, 2009.
- [9] K. Sassa, Y. Ashida, and T. Sugano, "Geophysical exploration for construction and disaster prevention technicians," Morikita Publishing, pp.117-127, Jun. 2007.
- [10] ASTM C 876-91, "Standard Test Method for Half-Cell Potentials of Uncoated Reinforcing Steel in Concrete," Annual Book of ASTM Standards, Vol.03.02, pp.457-462, 1999